COMPUTER METHODS IN APPLIED MECHANICS AND ENGINEERING 81 (1990) 1–11
NORTH-HOLLAND

SHOCKED TRANSONIC FLOW CALCULATIONS USING FINITE ELEMENTS AND A FICTITIOUS GAS

G.F. CAREY and T.T. PAN
Aerospace Engineering and Engineering Mechanics, University of Texas at Austin, U.S.A.

Received 2 March 1984

A variational finite element method for computation of shocked transonic flows is developed. The method combines the use of a fictitious gas for a regularized elliptic calculation together with the method of characteristics in the supersonic pocket. For shocked flows the shock condition is enforced using a penalty method in a dual 'two pass' algorithm which iteratively improves the calculated shock location. Comparison studies with experimental measurements and other numerical results for direct analysis codes are given for representative test cases.

1. Introduction

Finite difference methods for computing shocked transonic flows for both the full potential and small disturbance equations are now well established (see, e.g., [1–4]). There has also been some progress in developing finite element methods for compressible aerodynamic calculations see e.g. [5–8, 10]. Fung et al. [9] have employed the use of a fictitious gas and method of characteristics in finite difference calculations for design of shock-free transonic airfoils. Recently, we have developed these ideas in a finite element formulation and solution [6, 10]. Based on this analysis we develop here a further extension for computing shocked flows, which employs a penalty for the shock condition in a 'dual pass' algorithm in which the exterior subsonic flow, the supersonic pocket flow and shock location are iteratively improved. The technique appears most useful as an adjunct to shock-free airfoil design in which an appropriate shock-free airfoil is first designed and then the modified algorithm is used for off-design analysis.

Method

1. Governing equation

For steady inviscid compressible flow in two dimensions conservation of mass implies

$$\nabla \cdot (\rho \boldsymbol{q}) = 0 , \tag{1}$$

where $\rho = \rho(q)$ is the density and $q = |\boldsymbol{q}|$ is the velocity. The flow is considered to be uniform at upstream infinity and to remain isentropic in the presence of weak shocks.

Elsevier Science Publishers B.V. (North-Holland)

Using the adiabatic equation of state $p = k\rho^{\gamma}$ where p is the pressure, γ is the ratio of specific heats for the gas and k is a constant, and substituting in the Bernoulli equation of motion, we obtain the density–velocity relation

$$\rho = [\tfrac{1}{2}(\gamma + 1) - \tfrac{1}{2}(\gamma - 1)q^2]^{1/(\gamma - 1)}, \tag{2}$$

where we have normalized the density such that $\rho = 1$ at the reference sonic point $q = 1$. The flow is subsonic (elliptic) where $q < 1$ and supersonic (hyperbolic) where $q > 1$. Using (2) in (1) and setting $\boldsymbol{q} = \nabla\phi$, we obtain the full potential equation. Specification of the incident velocity in the far field, no flow across the body surface, a Kutta condition on a branch cut and the shock condition complete the mathematical statement of the problem [11].

The main steps in the following formulation consist of first solving a regularized elliptic problem by introducing a fictitious gas in the supersonic pocket, using the method of characteristics with the real gas and shock fitting in the supersonic pocket and finally iteratively resolving to improve the solution.

2. Regularized variational problem

The mixed (elliptic–hyperbolic) nature of the transonic flow equation leads to difficulties in constructing a standard variational statement and hence a finite element approximation. To circumvent this we first regularize the problem and construct a 'nearby' problem using a special class of fictitious gases defined by (2) with $-\infty < \gamma < -1$. The idea of a fictitious gas dates back to the early analytic studies of Chaplygin and Von Karman (see [12] for a discussion). In a previous study [6] we applied this approach to accelerate iterative solution of finite element solutions to subcritical and slightly supercritical (shock-free) flows. Fung et al. [9] and Dulikravich and Sobieczky [13] used the idea for a finite difference method in conjunction with the method of characteristics in the supersonic pocket to design shock-free airfoils. We have since introduced it in finite element calculations for shock-free airfoil design [14].

The shock-free airfoil problem is an inverse redesign problem in computational aerodynamics. The problem for a given airfoil is computed using a fictitious gas in the supersonic pocket to regularize the flow equations so that they remain elliptic. This is particularly important for finite element calculations since they are best suited to solution of elliptic rather than mixed problems. Having obtained the solution to the 'incorrect' but 'nearby' regularized elliptic problem, the method of characteristics may be applied from the sonic line using the real gas properties in the supersonic pocket to determine the redesigned airfoil (if it exists) which would produce the shock-free flow. The main attributes for the finite element method in this context are that it can be used to obtain solutions to the regularized elliptic problem on very general graded meshes in the physical flow domain.

In its present form however, this technique obviously cannot be applied to compute solutions to shocked flows for a given airfoil. We present here an extension of the above ideas to flows with weak shocks. Let us begin by immediately stating the regularized variational problem used in the following finite element analysis for flow with an imbedded shock: Find ϕ satisfying the essential boundary conditions and minimizing the functional

$$J = \int_{\Omega} [-\gamma(\tfrac{1}{2}(\gamma+1) - \tfrac{1}{2}(\gamma-1)q^2)^{\gamma/(\gamma-1)} - K]\, \mathrm{d}x\, \mathrm{d}y - \int_{\partial\Omega_2} \rho_\infty \boldsymbol{q}_\infty \cdot \boldsymbol{n}\phi\, \mathrm{d}s$$
$$+ \frac{1}{2\varepsilon} \int_{\partial\Omega_s} (\rho \boldsymbol{q}\cdot\boldsymbol{n} - \rho_s \boldsymbol{q}_s \cdot \boldsymbol{n})^2\, \mathrm{d}s\,, \tag{3}$$

where $\gamma = \gamma_1 > 1$, $K = 0$ for $q < 1$, and $\gamma = \gamma_2 = -1 - \beta$, $\beta > 0$, $K = 1/\gamma_1 - 1/\gamma_2$ for $q > 1$; the incident velocity $\boldsymbol{q}_\infty$ is specified on the far field boundary $\partial\Omega_2$ of the flow field Ω and $\partial\Omega_s$ denotes the shock line. The natural boundary condition is $\boldsymbol{q}\cdot\boldsymbol{n} = 0$ on the profile $\partial\Omega_1$. Note that the real gas $\gamma_1 > 1$ is used in the subsonic flow and the fictitious gas $\gamma_2 < -1$ is used in the local supersonic pocket. This class of fictitious gases differs from that used in finite difference shock-free calculations and is convenient to implement at the element level in our finite element calculations. The term K is introduced to improve the performance of the optimal control algorithm since the integrand in (3) is discontinuous across the sonic line. Here, for convenience and to elucidate the main argument, we have assumed a nonlifting profile so that the circulation Γ is zero and no Kutta condition is needed. The generalization to lifting profiles is quite straightforward [15].

The final term in (3) is a penalty term designed to enforce the shock condition

$$\rho \boldsymbol{q}\cdot\boldsymbol{n} = \rho_s \boldsymbol{q}_s \cdot \boldsymbol{n}\,, \tag{4}$$

which specifies that the normal mass flux is conserved across a shock line in the flow field. Parameter ε is the penalty parameter and (4) is satisfied as a constraint in the variational problem as $\varepsilon \to 0$. (See for example [10] for a discussion of finite element penalty methods for enforcing constraints). For subcritical flows and shock-free airfoil design calculations this term is omitted (i.e., set $\varepsilon^{-1} = 0$).

3. *Approximation of the regularized problem*

The first step in the solution scheme is to determine a finite element approximation to the regularized problem in (3). Accordingly, we define the finite element approximation space H^h of piecewise polynomials on a discretization of the domain Ω and seek the approximate potential $\phi_h \in H^h$ which makes $J(\phi_h)$ in (3) stationary for all admissible approximations from H^h. The solution is obtained using a conjugate gradient iteration, similar to that of Polak [16] and applied also by Bristeau et al. [17, 18], which is outlined briefly as follows:

(i) Given solution iterate $\phi_h^n \in H^h$, $n \geq 0$, determine the gradient direction g_h^n as the solution of the approximate variational problem

$$\int_{\Omega_h} \nabla g_h^n \cdot \nabla \eta_h\, \mathrm{d}x\, \mathrm{d}y = \int_{\Omega_h} \rho_h^n \nabla\phi_h^n \cdot \nabla\eta_h\, \mathrm{d}x\, \mathrm{d}y - \int_{\partial\Omega_h} \rho_\infty \boldsymbol{q}_\infty \cdot \boldsymbol{n}\eta_h\, \mathrm{d}s \quad \forall \eta_h \in H^h\,. \tag{5}$$

(ii) If $n = 0$ set $C_h^0 = g_h^0$ and go to (iii); that is, for the first iteration computation proceeds in the gradient direction; if $n > 0$ define the new conjugate gradient direction C_h^n by

$$C_h^n = g_h^n + \alpha^n C_h^n\,, \tag{6}$$

where

$$\alpha^n = \frac{\int_{\Omega_h} \nabla g_h^n \cdot \nabla (g_h^n - g_h^{n-1})\, dx\, dy}{\int_{\Omega_h} (\nabla g_h^{n-1})^2\, dx\, dy}\,. \tag{7}$$

(iii) Now construct the local minimizer: Find $\mu^n \in \mathbb{R}$, such that

$$J_h(\phi_h^n - \mu^n C_h^{n-1}) \leq J_h(\phi_h^n - wC_h^{n-1}) \quad \forall w \in \mathbb{R}\,,$$

where J_h is the finite element approximation of J in (3).

(iv) Adjust the solution

$$\phi_h^{n+1} = \phi_h^n - \mu^n C_h^n\,.$$

(v) Check convergence criteria and return to (i) or stop.

REMARK 1. For lifting profiles the circulation Γ is also adjusted iteratively by satisfying $\Gamma = [\![\phi]\!]$ at the trailing edge, where $[\![\cdot]\!]$ denotes the jump,

REMARK 2. For the minimization step (iii) we use functional evaluation with a quadratic fit to determine μ in subsequent numerical studies.

REMARK 3. A preconditioner to accelerate convergence of the conjugate gradient algorithm was also employed in the numerical studies.

As an indicative test of the solution algorithm, we compute pressure distributions on the airfoil surface for two subcritical flows ($\gamma_2 = \gamma_1 = \gamma$, $K = 0$, $\varepsilon^{-1} = 0$) in Figs. 1 and 2. In the first case the flow is for a (nonlifting) NACA 0012 airfoil at incident Mach number $M_\infty = 0.72$. Only the upper half flow field is discretized and the approximate solution is obtained using a graded mesh of linear triangular elements. The computed pressure coefficient compares favorably with the finite element results of Phares et al. [19] and experiments of Calspan in Vidal et al. [20]. The second case is for a lifting 82-06-09 airfoil at $M_\infty = 0.72$ and angle of attack $\alpha = -1.15$ degrees. Again, good comparison is obtained with experiments. The finite element results are for graded meshes of linear triangular elements containing 420 and 630 nodes, respectively.

4. *Local supersonic problem*

Having obtained the solution to the regularized supercritical flow problem, we proceed in the next step to introduce the method of characteristics to estimate the solution for the real gas in the supersonic pocket.

Consider the supersonic pocket $AI'C$ in Fig. 3, which is interpolated from the solution of the regularized transonic flow problem. Suppose I' is the point on the sonic line whose streamline is tangent to the supersonic pocket at only one point. Then the line segment AI'

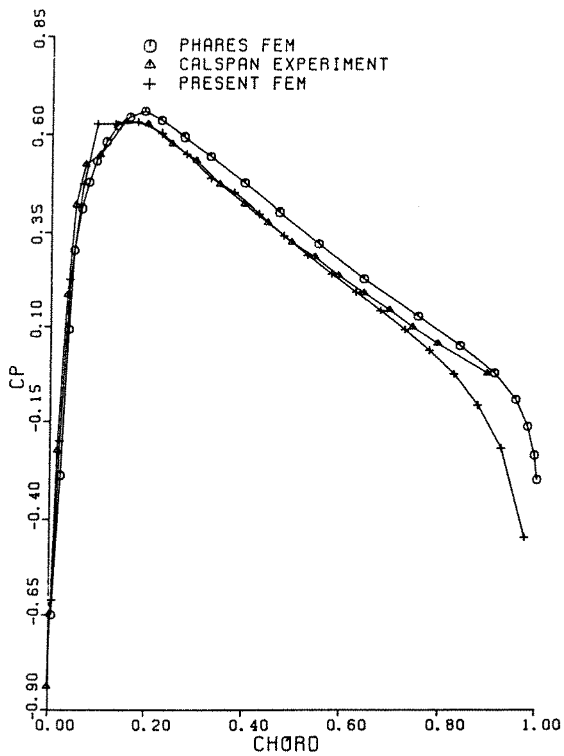

Fig. 1. Pressure distribution on a NACA 0012 airfoil at $M_\infty = 0.72$.

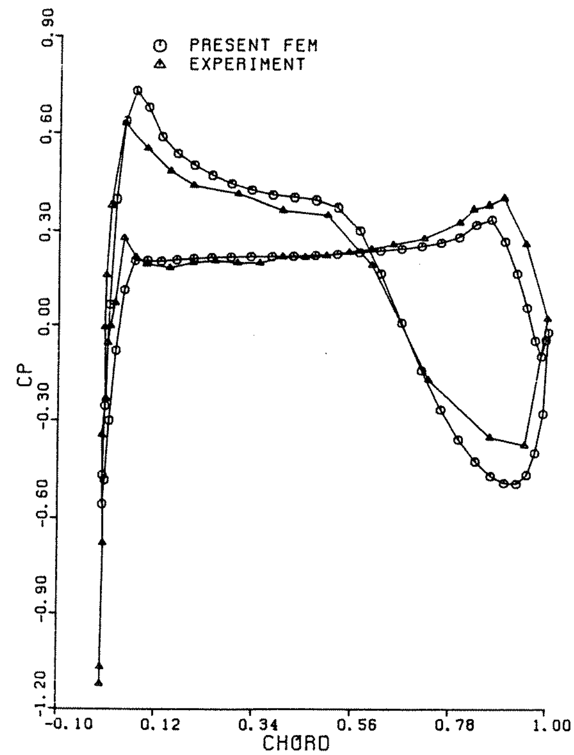

Fig. 2. Pressure distribution on a 82-06-09 airfoil at $M_\infty = 0.72$ and $\alpha = -1.15$.

must be a portion of the sonic line because an expansion shock is physically impossible and prohibited by the use of a fictitious gas. The other line segment $I'C$ could contain a shock wave or another portion of the sonic line (or both). We now have the following supersonic flow problem: Given the estimate of the sonic line segment AI' and the airfoil surface $\partial\Omega_1$, determine the unique supersonic flow field $AI'N'$, such that the boundary condition

$$\frac{\partial \phi}{\partial n} = 0 \quad \text{on } \partial\Omega_1$$

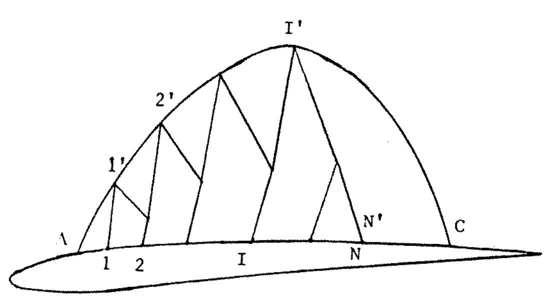

Fig. 3. The boundary and initial segment configurations for a supersonic flow problem.

is satisfied and the initial condition on the sonic line segment AI' is given from the solution of the regularized problem.

Let N points be chosen on the airfoil surface as shown in Fig. 3. We now compute the Ith expansion wave II' by the method of characteristics. Starting from the ith point on the airfoil surface (where the natural boundary condition is first enforced), we computed the ith expansion wave point-by-point using the immediate upstream conditions on the (I-1)th expansion wave until point I', the Ith point on the sonic line segment AI' or on the newly-determined shock boundary $I'N'$, is obtained. The computation is repeated for each expansion wave II', where $I = 1, 2, \ldots, N$, until the following condition on stream function ψ is satisfied at the point I':

$$\int_{C_1} \mathrm{d}\psi_{I'} = \int_{C_2} \mathrm{d}\psi_{I'}\,,$$

where C_1 and C_2 denote the directed curves AI' and II', respectively.

As the computation proceeds along the expansion wave II' line by line, the related compression wave is formed together with the expansion wave. The local flow direction on the sonic line segment AI' (i.e., the initial condition) is accordingly modified. Finally, the characteristic net $AI'N'$ is computed when the computation terminates at the point N' on the newly-developed shock boundary $I'N'$, within which a shock may be contained. Since the method of characteristics is employed to determine the flow field in our analysis, mass conservation is satisfied from upstream to downstream with appropriate consideration of the domain of dependence of the local supersonic flow.

5. *Iterative readjustment and algorithm*

This completes the second step in our dual pass algorithm. The potential at the shock line and mass flux across it can now be interpolated from the method of characteristics solution. This may then be used as data in the penalty term of the variational problem to compute a new regularized flow solution. Note that the shock position and data are fixed for this step of the algorithm and the sonic line and regularized flow are adjusted iteratively in the conjugate gradient scheme. The flow in the revised supersonic pocket is then recomputed using the corrected data on the adjusted sonic line and the real gas to obtain a revised shock location and shock data for the next pass. The entire process is then repeated to converge within a specified tolerance. In the following numerical experiments this algorithm was considered to have converged when the successive shock and sonic line calculations stabilized. Numerical experiments indicate that only 2 or 3 passes appear sufficient. One further point concerning the approach merits comment: Since the sonic line and shock constitute a free boundary in the flow separating the (real gas) subsonic flow and (real gas) supersonic pocket flow, this boundary must be computed iteratively as part of the flow solution. Numerical experiments for shock-free supercritical airfoils indicate that the location and shape of the supersonic pocket is not very sensitive to moderate changes in the choice of fictitious gas. For subcritical flows, we also recall that the Chaplygin gas ($\gamma = -1$) asymptotically is a reasonable approximation to the density relation of a real gas (see [12]). These observations suggest that the present iterative coupling will yield viable results for reasonable choices of γ and slightly supercritical flows with weak shocks. We shall see in later numerical comparisons with direct analysis programs that the solution behavior on the airfoil in the leading half of the supersonic flow pocket appears to be accurately characterized.

To summarize, the algorithm becomes:

(i) Solve the regularized problem on the whole domain Ω iteratively using a preconditioned conjugate gradient algorithm with coupled iterative evaluation of circulation Γ and using a fictitious gas in the supersonic pocket.

(ii) Use the method of characteristics to estimate the shocked local flow of the real gas in the supersonic pocket, thereby approximately determining the shock location and, consequently, the revised supersonic pocket.

(iii) Using the estimate of the supersonic domain from (ii) and the computed data for the shock, return to (i) and resolve. In this step, the shock data is fixed and the flow field and sonic line are adjusted accordingly. This solution provides adjusted data for (ii) and a corrected supersonic flow solution and shock are computed.

The above procedure is repeated until the position of the shock and sonic line converge within the mesh size used to approximate the domain.

Numerical results

In this section two numerical examples of nonlifting flows are computed to demonstrate the viability of the dual iterative method for shocked transonic flows. Shocks in these examples are naturally evolved during the associated iteration procedure. The capacity of the present method to predict a possible shock in the transonic flow field for an airfoil is illustrated and the accuracy of the shock prediction is examined by comparing the present numerical solution to available wind tunnel test data and solutions computed using different numerical methods.

The first problem is a circular cylinder of unit radius placed in a uniform incident flow with incident Mach number 0.45. Flow is from left to right and a graded mesh of approximately 500 linear elements is used to model the upper half flow field in each case. The second example is a NACA 0012 airfoil at zero angle of attack and for incident Mach number $M_\infty = 0.8$.

The characteristic net and shock line which completely define the shocked supersonic pocket on the upper half part of the object are displayed for both problems in Figs. 4 and 5, respectively. The region between the solid surface and the dotted sonic line is the shockless supersonic pocket interpolated from the solution of the first regularized transonic flow problem. The characteristic net and supersonic pocket with shock are computed from the initial value problem of Step (ii). In these two problems the shocked supersonic pocket is smaller than, and lies inside, the shockless supersonic pocket, and the shock is formed along the last reflected compression wave from the sonic line.

In the shocked supersonic pocket the domain of dependence of the local flow is appropriately considered by the method of characteristics. The computation always starts from the solid surface and proceeds along expansion waves from upstream to downstream in the flow. We observe that the boundary condition on the profile and the full potential equation are satisfied sequentially from upstream to downstream points and the flow pattern defined by the characteristic net in the supersonic pocket is uniquely determined. The numerical scheme

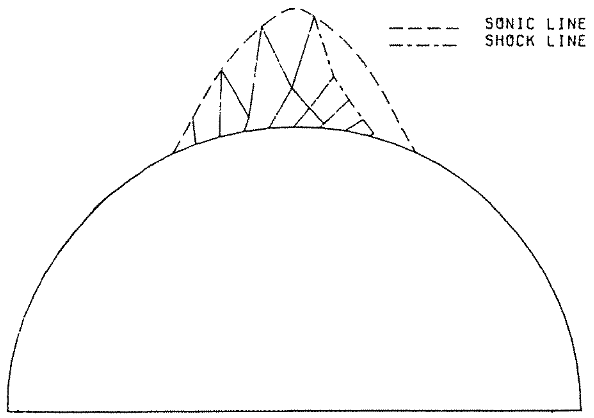

Fig. 4. The characteristic net, sonic line and shock line for a circular cylinder at $M_\infty = 0.45$.

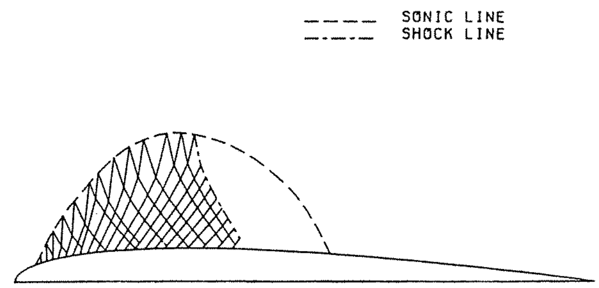

Fig. 5. The characteristic net, sonic line and shock line for a NACA 0012 airfoil at $M_\infty = 0.80$.

performs reasonably well, even in the case of the blunt cylinder in which the local supersonic flow direction is significantly different from the free stream flow direction.

We now present numerical solutions in the form of computed pressure distributions on the profile surface for these two problems and compare them with the results computed using the least-squares finite element method of Bristeau et al. [17]. For the cylinder, a sharp shock is obtained from both methods as indicated in Fig. 6, and the results agree well on the surface except for a small highly supersonic region, where a strong suction force is predicted and a sharper shock is produced by the present method. The slight discrepancy here may possibly be attributed to using too few nodes on the cylinder surface inside the supersonic pocket in our computation. The mesh in the supersonic region is insufficient and hence the numerical errors produced upstream are propagated downstream. At the extreme downstream end of the supersonic pocket this leads to the discrepancy noted and a sharper shock. This discrepancy and the shock strength may be improved by constructing a finer characteristic net in the supersonic pocket as will be seen in the following example. The general agreement of the solutions, particularly in the forward part of the supersonic region indicates that the present scheme is capable of producing viable solutions to the weakly shocked transonic flow problem and that the fictitious gas regularization gives a reasonable approximation to the leading part of the sonic line.

Results from the present method are computed using a finer characteristic net in the supersonic pocket for a NACA 0012 airfoil than that for the preceeding cylinder example and compared with other results in Fig. 7. We observe that a weak shock appears on the airfoil surface with a strength equally-well predicted from both methods. However, for this more slender profile there is a notable discrepancy in the shock position which warrants further comment. If we compare results of the present method with those of the experiment in Fig. 7 [20], we find better agreement of shock location and strength than obtained using a typical conservative finite difference method due to Jameson [3]. These results, however, may be somewhat misleading and are open to interpretation: First, the experimental results include viscous effects whereas neither numerical model has accomodated the boundary-layer. Second, and perhaps more important, the finite difference results are for a conservative scheme.

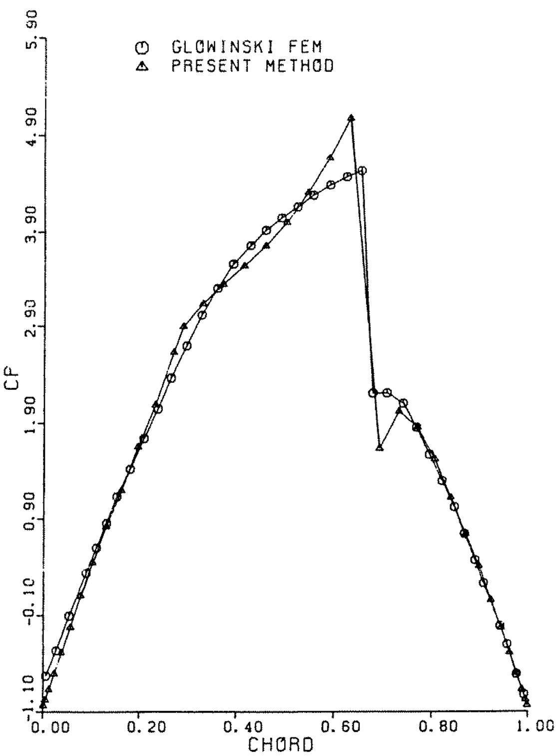

Fig. 6. Pressure distribution on a circular cylinder at $M_\infty = 0.45$.

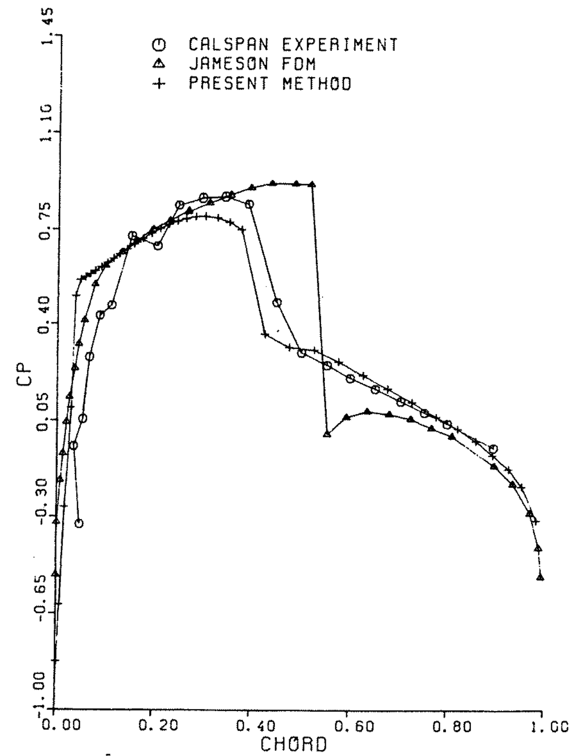

Fig. 7. Pressure distribution on a NACA 0012 airfoil at $M_\infty = 0.8$ and $\alpha = 0$.

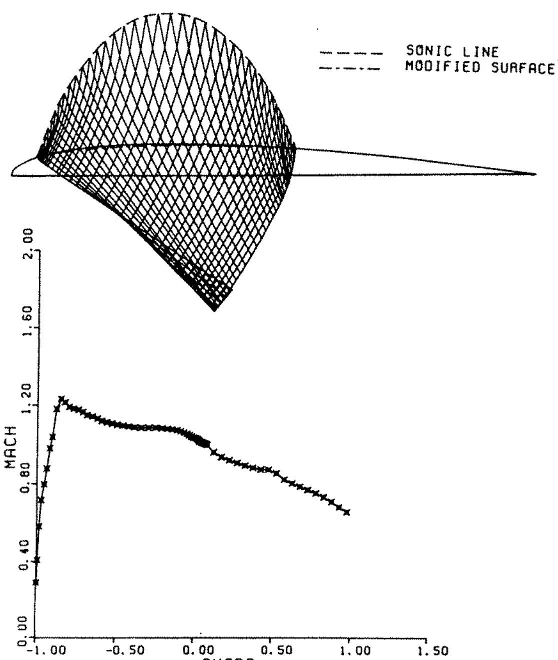

Fig. 8. Pressure distribution on a modified shockless NACA 0012 airfoil at $M_\infty = 0.8$ and $\beta = 9$.

It is now generally recognized that nonconservative methods give better agreement with experiment and with results using the Euler equations. We conjecture here that the effect of the penalty term on the shock relation in our formulation and also iteratively uncoupling the supersonic flow with the characteristics fit to the shock may have effects similar to a nonconservative method or Euler code.

Concluding remarks

The foregoing finite element formulation together with the method of characteristics and shock fitting has been developed and applied successfully to representative test problems. The method is an extension of the use of fictitious gas regularization techniques which have previously been developed for shock-free airfoil design: in the shock-free redesign analysis the regularized flow in Step (i) of the algorithm is computed as before but now in Step (ii) the initial-value problem is again solved from the sonic line ignoring the presence of the profile boundary. The zero streamline contour gives the modified airfoil shape corresponding to the shock-free flow. The modified surface for a sample problem and the redesigned shock-free airfoil are shown in Fig. 8 (see [9, 14] for further discussion of shock-free design).

While we have demonstrated here the applicability of the method for shocked flow calculations, it is not advocated as an alternative to other direct analysis methods. Rather, the present analysis seems most useful in conjunction with shock-free redesign studies, where the shock-free design is first made using this regularization technique and then off-design studies of the redesigned airfoil are computed.

References

[1] E.M. Murman and J.D. Cole, Calculation of plane steady transonic flows, AIAA J. 9 (1) (1971).

[2] T.L. Holst and W.F. Ballhaus, Conservative implicit schemes for the full potential equation applied to transonic flows, NASA–TM–78469, March 1978.

[3] A. Jameson, Transonic potential flow calculation using conservative form, Proc. AIAA 3rd Computational Fluid Dynamics Conf., Hartford, CT, June 1975.

[4] M. Nakamura, A method for obtaining shockless transonic flows past airfoils, partially modified from a given arbitrary airfoil, NAL TR-602, February 1980.

[5] G.F. Carey, Variational principles for the transonic airfoil problem, Comput. Methods Appl. Mech. Engrg. 13 (1978) 129–140.

[6] G.F. Carey and T.T. Pan, Computation of subcritical compressible fluid flow, Comput. & Fluids 9 (1979) 33–41.

[7] A. Eberle, Finite element methods for the solution of full potential equation in transonic steady and unsteady flow, Proc. 3rd Internat. Symp. on Finite Elements in Flow Problems, Banff, Canada, June 1980.

[8] A. Ecer and H.U. Akay, Treatment of shocks in the computation of transonic flows using finite elements, Proc. 3rd Internat. Symp. on Finite Elements in Flow Problems, Banff, Canada, June 1980.

[9] K.Y. Fung, H. Sobieczky and R. Seebass, Numerical aspects of the design of shock-free wings, AIAA paper 79–1557, 1982.

[10] G.F. Carey and J.T. Oden, Finite Elements: Fluid Mechanics (Prentice-Hall, Englewood cliffs, NJ, 1983).

[11] A.H. Shapiro, The Dynamics and Thermodynamics of Compressible Fluid Flow, Vols. I and II, Ronald Press Co., New York, 1958.

[12] R. Von Mises, Mathematical Theory of Compressible Fluid Flow (Academic Press, New York, 1958).

[13] D.S. Dulikravich and H. Sobieczky, CAS22-FORTRAN program for fast design and analysis of shock-free airfoil cascades using fictitious gas concept, NASA report 3507, January 1982.

[14] T.T. Pan and G.F. Carey, Shock-free redesign using finite elements, Comm. Appl. Numer. Methods 2 (1986) 29–35.

[15] T.T. Pan, Computation of compressible flows using finite elements and optimization techniques, Ph.D. Dissertation, The University of Texas at Austin, 1983, University Microfilms, Ann Arbor, Michigan, 48106.

[16] E. Polak, Computational Methods in Optimization (Academic Press, New York, 1971).

[17] M.O. Bristeau, R. Glowinski, J. Periaux, P. Perrier, O. Pironneau and G. Poirrier, Application of optimal control and finite element methods to the calculation of transonic flows and incompressible viscous flows, IRIA-294, April 1978.

[18] M.O. Bristeau, R. Glowinski, J. Periaux, P. Perrier, O. Pironneau and G. Poirrier, Transonic flow simulations by finite elements and least square methods, Proc. 3rd Internat. Symp. on Finite Elements in Flow Problems, Banff, Canada, June 1980.

[19] W.J. Phares and K.R. Kneile, Solution to the Eulerian equations by the finite element method with an application to transonic flow, ARO Inc. AEDC-TR-76-86, 1976.

[20] R.J Vidal, P.A. Catlin and D.W. Chudyk, Two-dimensional subsonic experiments with a NACA 0012 airfoil, CALSPAN Report No. RK-5070-A-3, December 1973.